A dynamic multibody model of the physiological knee to predict internal loads during movement in gravitational field

Simone Bersini[a,b]*, Valerio Sansone[c,d1] and Carlo A. Frigo[e2]

[a] *Laboratory of Biological Structure Mechanics, Gruppo Ospedaliero San Donato Foundation, Via Riccardo Galeazzi 4, Milano 20161, Italy;* [b] *Department of Electronics, Information and Bioengineering, Politecnico di Milano, Milano, Italy;* [c] *Dipartimento di Ortopedia e Traumatologia, Università degli Studi di Milano, Milano, Italy;* [d] *IRCCS Istituto Ortopedico Galeazzi, Via Riccardo Galeazzi 4, Milano 20161, Italy;* [e] *Biomechanics and Motor Control Laboratory, TBM Lab, Department of Electronics, Information and Bioengineering, Politecnico di Milano, Via Golgi 39, Milano 20133, Italy*

Obtaining tibio-femoral (TF) contact forces, ligament deformations and loads during daily life motor tasks would be useful to better understand the aetiopathogenesis of knee joint diseases or the effects of ligament reconstruction and knee arthroplasty. However, methods to obtain this information are either too simplified or too computationally demanding to be used for clinical application. A multibody dynamic model of the lower limb reproducing knee joint contact surfaces and ligaments was developed on the basis of magnetic resonance imaging. Several clinically relevant conditions were simulated, including resistance to hyperextension, varus–valgus stability, anterior–posterior drawer, loaded squat movement. Quadriceps force, ligament deformations and loads, and TF contact forces were computed. During anterior drawer test the anterior cruciate ligament (ACL) was maximally loaded when the knee was extended (392 N) while the posterior cruciate ligament (PCL) was much more stressed during posterior drawer when the knee was flexed (319 N). The simulated loaded squat revealed that the anterior fibres of ACL become inactive after 60° of flexion in conjunction with PCL anterior bundle activation, while most components of the collateral ligaments exhibit limited length changes. Maximum quadriceps and TF forces achieved 3.2 and 4.2 body weight, respectively. The possibility to easily manage model parameters and the low computational cost of each simulation represent key points of the present project. The obtained results are consistent with *in vivo* measurements, suggesting that the model can be used to simulate complex and clinically relevant exercises.

Keywords: knee model; multibody dynamics; knee ligaments; knee internal loads

1. Introduction

Knee joint kinematics is determined by a complex interaction of forces produced in the contact areas of the tibio-femoral (TF) and patello-femoral joints through the action of active (muscles) and passive (ligaments, capsule) elements.

Despite a considerable loading of the internal structures (Taylor and Walker 2001; Kutzner et al. 2010), the physiological knee maintains its ability to flex-extend during body support as well as during swinging. The geometry of the articular surfaces and the arrangement of ligaments and tendons are critical to preserve these functional characteristics.

Models attempting to describe knee joint kinematics and loading are numerous (Andriacchi et al. 1983; Gill and O'Connor 1996; Li et al. 2002). However, most models adopt rather crude simplifications of plane of movement, internal structures and joint surfaces (Shelburne and Pandy 1997; Abdel-Rahman and Hefzy 1998; Koehle and Hull 2008), and are designed for quasi-static conditions (Bei and Fregly 2004). Quite detailed analysis of internal structures can be performed by integrating multibody models with finite element methods (Bendjaballah et al. 1995; Beillas et al. 2004; Papaioannou et al. 2008). However, difficult definition of the constitutive equation parameters for soft tissue under dynamic large deformations represents a limit to this approach. Furthermore, the complexity of these models requires huge amount of computational resources, and this makes testing of different loading conditions and movements quite challenging. For clinical application, instead, it would be advisable to obtain information about TF contact forces, ligament deformations and loads for a number of daily life motor tasks (walking, jumping, stair climbing, getting up from a chair and sitting) in a simple though accurate way, and to have the possibility to simulate changes of some geometrical and mechanical parameters. These data would be useful to better clarify the aetiopathogenesis of knee joint diseases (Lane and Thompson 1997), the function of ligaments (Fishkin et al. 2002) and the effects generated by the surgical reconstruction of ligaments or by knee joint arthroplasty procedures (Thompson et al. 2011). Moreover, they could influence prosthetic design (Insall and Kelly 1986) and help to define proper implantation parameters.

*Corresponding author. Email: simone.bersini@grupposandonato.it

With these objectives in mind, we have developed a multibody dynamic model that realistically represents knee joint anatomy and function, still remaining manageable in terms of number of input parameters and computational resources. The model implements the nonlinear properties of soft tissues and is able to predict relative movements of bones under loading, ligament stretching and forces, and TF contact forces in a gravitational field.

2. Materials and methods

2.1 Model generation

A magnetic resonance imaging (MRI) scan was obtained from a Caucasian male [age: 42 years; body height (BH): 1.76 m; body mass (BM): 72.6 kg], lying supine. Images were captured at 1-mm slice thickness and were processed through a reconstruction software (Amira 5.3.3, Visage Imaging, Inc., San Diego, CA, USA) in order to create three-dimensional (3D) models of pelvis, femur, patella, tibia and fibula. A multibody dynamic model (Figure 1) was generated using one of the commercially available software packages (Working Model 3D, MSC, Software Corp., Santa Ana, CA, USA) that have the capability to solve forward dynamics in complex articulated systems of rigid bodies (Brunner et al. 2008; Frigo et al. 2010). Integration of differential equations was based on Kutta–Merson method (integration time: 0.010 s).

The femur was connected to the pelvis through a spherical joint representing the hip. Tibia and fibula were rigidly connected to one another so that they constituted a single rigid body. The foot was just designed as a polyhedron to complete the lower limb and to interface tibia and ground during some exercises. The connection between tibia and foot, the ankle, was modelled as a two joints system: (1) talo-crural joint, cylindrical, medio-laterally oriented, to allow dorsi-plantar flexion; (2) sub-talar joint, cylindrical, antero-posteriorly oriented, to allow inversion–eversion. An additional cylindrical joint, longitudinally oriented, was added to allow tibial internal–external rotation. The knee joint was defined by the contact between femoral condyles and tibial plateau, and was constrained by forces due to anterior cruciate ligament (ACL), posterior cruciate ligament (PCL), lateral collateral ligament (LCL) and medial collateral ligament (MCL). The patella was modelled as a cylinder in contact with the femoral groove, and was constrained to the tibia by an unextendable cord representing the patellar tendon. Two springs were added at the two sides of the patella in order to represent the alar ligaments. At the upper edge the patella was connected to a force generator, representing the quadriceps muscle, through a chain of three short cylinders that modelled the quadriceps tendon. These cylinders could come into contact with the femoral trochlea during knee flexion, thus reproducing the physiological wrapping of the quadriceps tendon over the femoral groove.

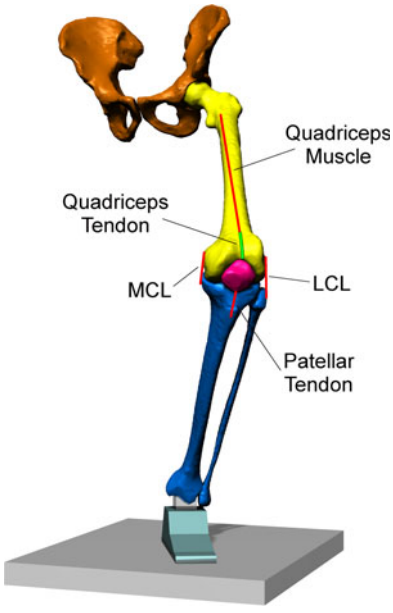

Figure 1. The multibody dynamic model. Structure of the lower limb and considered anatomical segments.

In order to obtain a proper sliding between the contact surfaces, femoral condyles and tibial plateau were smoothed by means of a CAD software (Rhinoceros 4.0, McNeel, Seattle, WA, USA). The distance between points lying on the original surface and the corresponding points of the smoothed surface did not exceed 0.5 mm (Figure 2). The interaction between contact surfaces was modelled as an inelastic collision. Friction coefficient was set at 0.02 (Shrive and Frank 2005). The masses of pelvis, thigh, lower leg and foot were determined from anthropometric data (Clauser et al. 1969) (Table 1).

2.2 Ligament properties

Ligament and tendon attachment points were defined as the centroids of the respective attachment areas derived from our MRI images with the help of anatomical atlases.

According to Blankevoort and Huiskes (1991), ligaments were assumed to be elastic with a nonlinear force–strain relationship described by a piecewise function:

$$f = \begin{cases} 0.25k\frac{\in^2}{\in_l}, & 0 \le \in \le 2\in_l, \\ k(\in - \in_l), & \in > 2\in_l, \\ 0, & \in < 0, \end{cases} \quad (1)$$

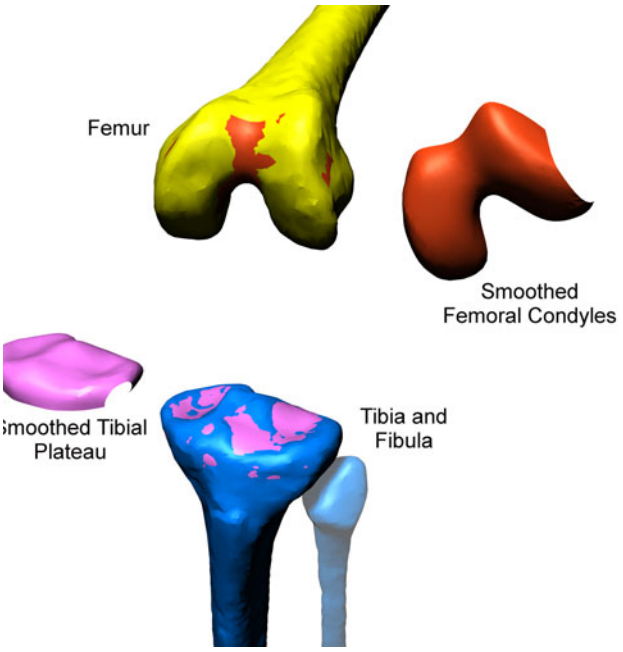

Figure 2. Surface reconstruction of proximal tibia and distal femur. The distance between the smoothed surfaces and the original ones does not exceed 0.5 mm in the useful contact area.

where f is the tensile force, k is the ligament stiffness and $\in$ is the strain in the ligament computed from its actual length L and the zero-load length L_0. The $\in_l$ parameter was assumed to be 0.03 (Blankevoort and Huiskes 1991).

If the ligament strain was $< 2\,\in_l$, then the ligament force was a quadratic function of the ligament strain; a linear relationship resulted when the ligament strain was $> 2\,\in_l$. At the reference (full extension) position of the joint, the initial strain $\in_r$ was assumed for each ligament on the basis of numerical data provided by Blankevoort and Huiskes (1991). This parameter allowed us to determine the zero-load length, since the reference length was known from the initial (extended) position of the model:

$$L_0 = \frac{L_r}{\in_r + 1}. \qquad (2)$$

Table 2 reports stiffness values, based on data obtained by Shelburne and Pandy (1997), as well as ligament zero-load lengths and initial strain values for each ligament.

Ligaments were divided into multiple bundles to analyse their specific function: the ACL and the PCL were simulated considering anterior (aACL, aPCL) and posterior (pACL, pPCL) bundles. The MCL was designed by considering an anterior superficial bundle (aMCL), an intermediate superficial bundle (iMCL) and a deep posterior bundle (dMCL). The LCL was represented as a single ligament unit.

Table 1. Anthropometric and inertia parameters referred to our model subject: BM = 72.6 kg; BH = 1.72 m.

Body segment	Mass ratio (%)	Mass (kg)	$J_{x(A/P)}$ (kgm^2)	$J_{y(M/L)}$ (kgm^2)	$J_{z(Long)}$ (kgm^2)
Pelvis	15.8	11.5	0.0493	0.0268	0.0457
Thigh	10.3	7.5	0.0877	0.0877	0.013
Lower leg	4.4	3.2	0.0362	0.0362	0.00324
Foot	1.5	1.1	0.000839	0.00266	0.00233

Notes: J_x, J_y and J_z are the moments of inertia of the considered body segments with reference to anterior/posterior (A/P), medio-lateral (M/L) and longitudinal (Long) axes, respectively.

2.3 Validation and simulations

The model was first initialized in a standing upright posture and then it was tested in a series of paradigmatic conditions: (1) free hung; (2) free flexion–extension; (3) resistance to hyperextension; (4) varus–valgus stability. In addition, the clinical tests of anterior and posterior drawer were simulated having the knee fully extended or flexed at 90°. In all these trials, the gravity field was applied. Quadriceps force, which should be zero in these conditions, was set to a small value, 50 N, just to keep the patellar tendon in contact with the femoral trochlea. A squat movement was then simulated and the equilibrium forces of quadriceps, ligaments, and TF contacts were computed.

2.4 Initialization

Initialization was performed while femur and tibia were vertically aligned. The foot was fixed on the floor and the

Table 2. Values of stiffness (K), zero-load length (L_0), reference length (L_r) and initial strain ($\in_r$) assumed in the model for each ligament bundle.

Ligament	K (N)	L_0 (mm)	L_r (mm)	$\in_r$
aACL	1500	32.3	34.6	0.07
pACL	1600	24.4	26.8	0.1
aPCL	2600	30.4	27.4	−0.1
pPCL	1900	31.5	32.1	0.02
aMCL	2500	86.9	93	0.07
iMCL	3000	90.6	96.9	0.07
dMCL	2500	34.1	36.3	0.065
LCL	2000	53.1	56.5	0.065

Notes: Abbreviations in the table are as follows: aACL and pACL, anterior cruciate ligament (anterior and posterior bundle); aPCL and pPCL, posterior cruciate ligament (anterior and posterior bundle); aMCL and iMCL, medial collateral ligament (anterior and intermediate superficial bundle), dMCL, medial collateral ligament (deep posterior bundle); LCL, lateral collateral ligament.

pelvis was allowed to slide along a vertical axis. A vertical load of 300 N was applied to the hip, which was obtained as the half body weight minus one lower limb, increased by 25% to take into account a possible asymmetrical loading. Ligament reference lengths L_r were set, as a first guess, corresponding to the unloaded condition. Small adjustments of bone orientation and ligament length were produced by the load. Ligament reference lengths were then reset in the new position and a second readjustment was observed. After the third iteration, the adaptive changes in ligament length were <0.1 mm, and the corresponding bone positions and ligament lengths were assumed as the reference (Table 2).

2.5 *Paradigmatic conditions*

The free hung condition was checked by fixing the femur in the vertical alignment and releasing the foot from the ground. Few small oscillations occurred, until the tibia achieved a position corresponding to a slightly flexed knee joint (6°). Contact force and ligament forces were computed in this final position. To check free flexion under gravity, femur and tibia were positioned horizontally and the femur was fixed. The tibia was then let free to oscillate. We stopped the movement in a position corresponding to the free hung equilibrium, 96°, and measured the forces in that position. Then, the femur was positioned vertically while the knee was flexed at the same angle (tibia 6° above horizontal). The subsequent knee extension produced by gravity was analysed. To check hyperextension and varus–valgus stability the model was placed horizontally in three different lying orientations: prone, on the right side and on the left side. Anterior–posterior drawer was simulated by applying a forward–backward displacement of ± 5 mm, while the leg was prevented to rotate. The knee was either extended at 0° or flexed at 90°. The femur was constrained by a rigid joint to the background. The force required to produce anterior and posterior displacement of the tibia was measured at the level of the femoral constrain. These paradigmatic conditions are depicted in Figure 3.

2.6 *Squat movement*

The squat exercise was simulated starting from the upright position adopted for the model initialization. The range of movement from 0° (full extension) to 90° was travelled by imposing a 10°/s angular velocity to the talo-crural joint. Quadriceps force was increased according to a sigmoid function of the knee joint angle, from 200 to 900 N, in order to keep an internal ligament tension. Then, in a discrete number of fixed positions (0°, 15°, 30°, 40°, 50°, 60°, 75°, 90° flexion angle), the quadriceps force was progressively increased up to a level that was able to sustain the load in a quasi-static condition.

Ligament forces and elongations, quadriceps force and TF contact forces were extracted from the model in each of these positions.

3. Results

3.1 *Free hung, free flexion–extension, hyperextension and varus–valgus*

The developed model was both able to transmit the body weight to the floor when the knee was extended and to swing when the foot was suspended from the ground. The magnitude of the longitudinal contact force computed in the free hung condition at the end of the free oscillations was 272 N (Table 3). All the ligaments except the PCL exhibited a force. At the end of the free flexion, instead, when the femur was horizontal, the ACL was completely unloaded while a force was developed by the PCL. It is worth noting that free flexion occurred in a plane that was not vertical, because the lateral condyle had a greater anterior–posterior length than the medial condyle. For this reason the foot, when the knee was flexed at approximately 90°, was positioned medially with respect to the knee, and the shank was oriented at approximately 20° in relation to the vertical. In this condition the MCL, iMCL and dMCL exhibited the highest tensions, while the LCL was unloaded (Table 3). When the knee was let free to extend, starting from approximately 90° of flexion, femur vertically oriented, a large oscillation occurred that forced the knee to hyperextend by approximately 30° (this phenomenon will be discussed later). In this position, the longitudinal TF contact force was extremely high (2180 N, 3 times body weight (BW)) and was in relation to a very high tension in all the ligaments.

When the model was set in a prone orientation, with the femur horizontal, the knee reached a hyperextension of 10.5°. The most stressed ligaments were the ACL, MCL and LCL. When the model was set lying on the right side the knee, belonging to the left side, was forced to varus and tended to flex. At equilibrium (20° of flexion) the most stressed ligaments were the ACL and LCL. No tension was obtained in the PCL. When the knee was forced to valgus (model lying horizontally on the left side), the tendency to flex was very mild (1°). The most stressed ligaments were the different MCL components and ACL as a whole.

3.2 *Anterior–posterior drawer*

The force required to draw the tibia forward by 5 mm was higher when the knee was extended than when it was flexed (Table 4). In both exercises the ACL was tensed, and its force was considerably high (392 N) when the knee

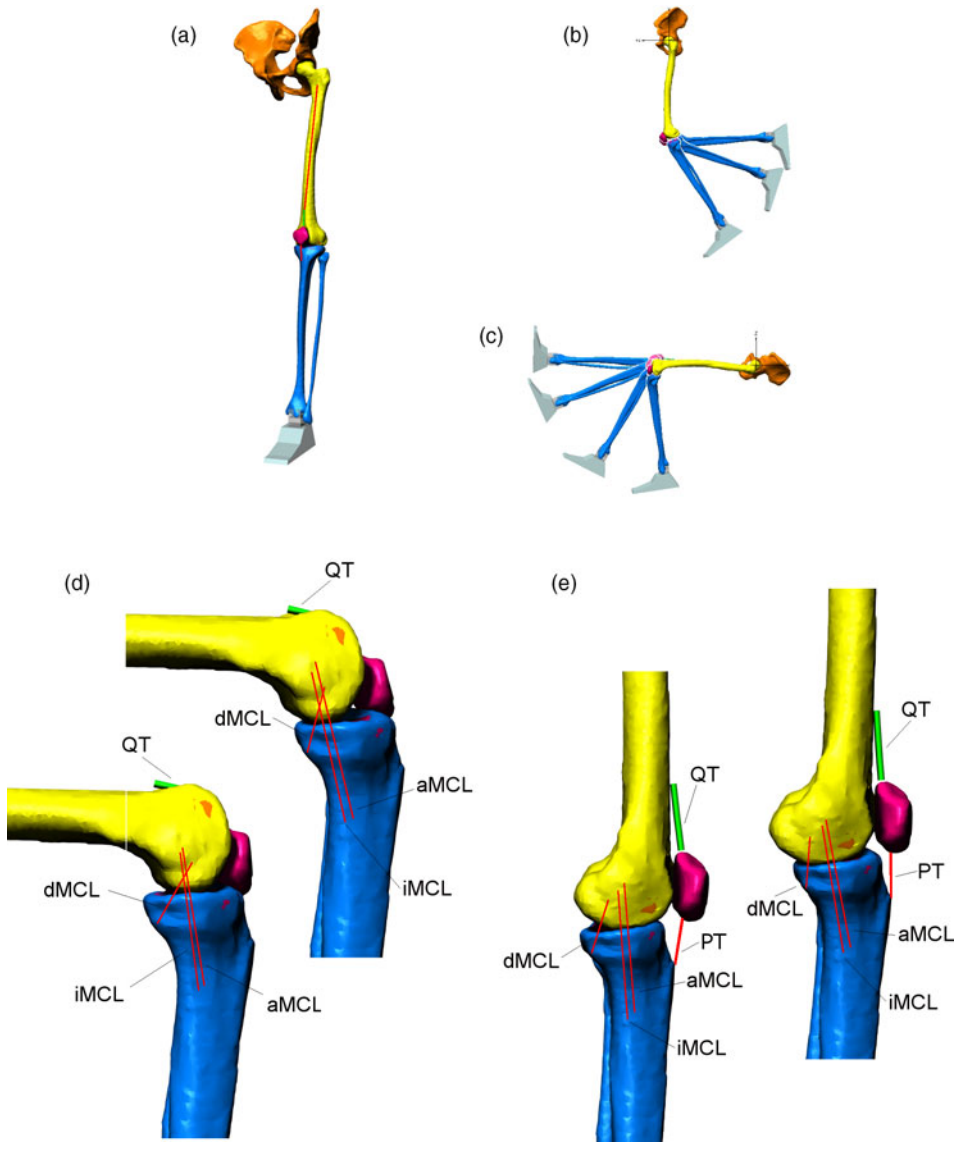

Figure 3. Paradigmatic conditions tested: (a) free hung, (b) free extension, (c) free flexion, (d) posterior–anterior drawer (flexed knee) and (e) posterior–anterior drawer (extended knee). aMCL, anterior superficial bundle of the MCL; iMCL, intermediate superficial bundle of the MCL; dMCL, deep posterior bundle of the MCL; PT, patellar tendon; QT, quadriceps tendon.

was extended. Posterior drawer, instead, produced a significant load on PCL, higher with knee flexed (319 N) and lower with knee extended. MCL bundles were loaded in all these testing conditions, with the highest values achieved in the anterior drawer, knee flexed condition. dMCL achieved its highest tension during posterior drawer tests.

3.3 Squat movement

The quadriceps force during a squat movement, starting from full extension to a flexion angle of 90°, is reported in Figure 4. The force was very small at 15° and reached 2300 N (3.2 BW) at 90° of flexion. The slope of the curve was slightly higher in the range 15–40° than in the range 60–90°. The TF contact force increased with flexion in a nonlinear way: after an initial rise it stayed almost constant until 45°, then it arose up to a value of 2990 N (4.2 BW). Anterior–posterior and medio-lateral components, not reported in Figure 4, were approximately 20% of the total contact force.

All cruciate ligament bundles, except the aACL, shortened during the first 40° of flexion. Then, PCL bundles lengthened while ACL bundles shortened (Figure 5(a)). As a consequence, the force in the ACL components (Figure 5(b)) was present in the first part of the knee flexion, up to 30–50°, while the force in the PCL was present in the second part, beyond 50° of flexion.

Table 3. Force magnitude (N) in the joint structures obtained in six paradigmatic conditions (see text).

	Free hung (6° flex.)	Free flexion (96° flex.)	Free extension (33° ext.)	Hyperextension (10.5° ext.)	Varus 7.7° (20.8° flex., 2.4° int. rot.)	Valgus 0° (0.9° flex., 1.3° int. rot.)
TF Long	272	496	2180	891	282	437
TF A/P	124	43.9	189	159	59.5	129
TF M/L	0.1	124	538	96.9	27.9	54
aACL	46.4	0	276	126	22.9	70.1
pACL	81.4	0	564	236	72.2	93
Tot. ACL	127.8	0	840	362	95.1	163.1
aPCL	0	78.8	23.4	70.2	0	0
pPCL	0	0	369	0	0	0.03
Tot. PCL	0	78.8	392.4	70.2	0	0.03
aMCL	79.6	141	147	122	47.9	99.3
iMCL	90.5	123	206	152	45	117
Tot. MCL	170.1	264	353	274	92.9	216.3
dMCL	22.1	104	240	97.6	0.9	61.3
LCL	52.8	0	645	223	109	42.2

Notes: TF Long, TF A/P and TF M/L represent TF contact forces in the longitudinal, anterior–posterior and medio-lateral direction, respectively. Ext., extension; flex., flexion; int. rot., internal rotation.

As to the collateral ligaments, the aMCL and iMCL changed their length very slightly (Figure 5(c)), and their force increased also slightly with increasing flexion angle (Figure 5(d)). The dMCL, instead, increased its length more considerably, particularly in relation to its short initial length, so that the force it generated reached about 400 N (Figure 5(d)), which was the highest ligament force recorded in our simulations. LCL appeared to shorten with knee flexion and its force decreased quite rapidly in the first 15° of flexion.

4. Discussion

Biomechanical models adopted to estimate the internal loads of the knee joint are usually based on quite a rough simplification of the TF contact surfaces (Gill and O'Connor 1996; Shelburne and Pandy 1997). Our model is the first one, to our knowledge, that uses the original contact surfaces, obtained from MRI, to simulate the TF interaction and to predict internal loads in a set of dynamic conditions which include suspended oscillations as well as body support. The relative position of bones is the result of contact forces developed between femoral condyles and tibial plateau, femoral trochlea and patella, quadriceps tendon and femoral trochlea, and ligaments attached at predefined positions on femur and tibia. No other constraints were applied to the model, and the linkage with the ground, for movements including body weight support, was designed to reproduce the physiological degrees of freedom of the ankle joint, in order to avoid the generation of internal forces at the knee joint due to unrealistic external kinematic constraints.

The obtained kinematics and forces were quite realistic in all simulations, although the effect of some simplifications appears in specific test conditions. Particularly, during free extension, the movement of the lower leg continues beyond the physiological knee extension range, up to approximately 30° of hyperextension. This phenomenon is surely due to the absence of energy dissipation components. In all likelihood, the addition of other elements in the rear side (joint capsule and flexor muscles) with incorporated viscous properties would help to reduce the momentum at the end of knee extension. Another simplification was the limited dimension of the reconstructed condyle surface that can support interaction forces with the tibia, and the absence of menisci: this simplification excludes the possibility to obtain accurate contact forces beyond 100° of flexion. However, this limit does not affect the results of the squat movement, that was limited to 90° of flexion, nor future applications concerning walking or stair climbing, in which the

Table 4. Force magnitude (N) in the joint structures obtained during simulated drawer tests.

	Knee flex., ant. drawer	Knee flex., post. drawer	Knee ext., ant. drawer	Knee ext., post. drawer
Drawer force	226	298	328	138
aACL	50.2	0	181	3.38
pACL	0	0	211	71.1
Tot. ACL	50.2	0	392	74.48
aPCL	1.18	319	0	4.57
pPCL	0	0	0	106
Tot. PCL	1.18	319	0	110.57
aMCL	188	138	115	91.6
iMCL	168	131	126	109
Tot. MCL	356	269	241	200.6
dMCL	98	264	12.8	140
LCL	0	0	30.8	116

Notes: Ant., anterior; post., posterior; flex., flexion; ext., extension.

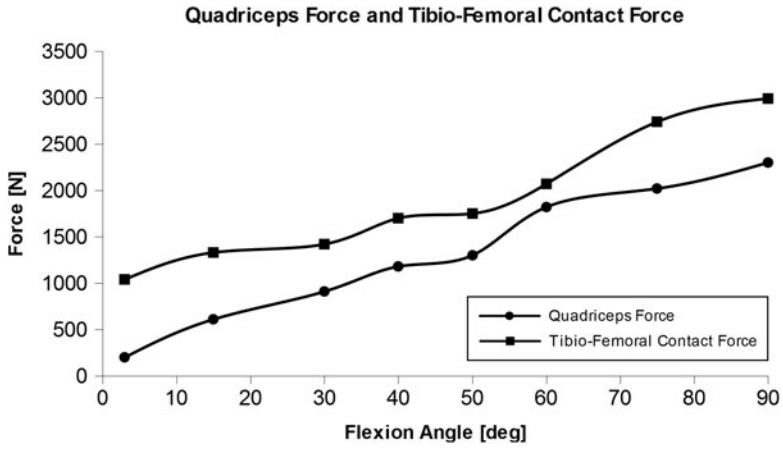

Figure 4. Forces produced by the quadriceps muscle and measured at the TF contact at various angles of knee flexion during a squat motor task.

maximum flexion angle is usually less that 100° (Riener et al. 2002). Again, the patello-femoral joint was represented by a cylinder in contact with the femoral grove. This simplification was aimed at reducing the simulation time, and was considered adequate to our purpose, that was to implement the structure of the extension mechanism of the knee. This simplification, however, prevents us to obtain a reliable measure of the patello-femoral contact force, which in fact has not been reported here.

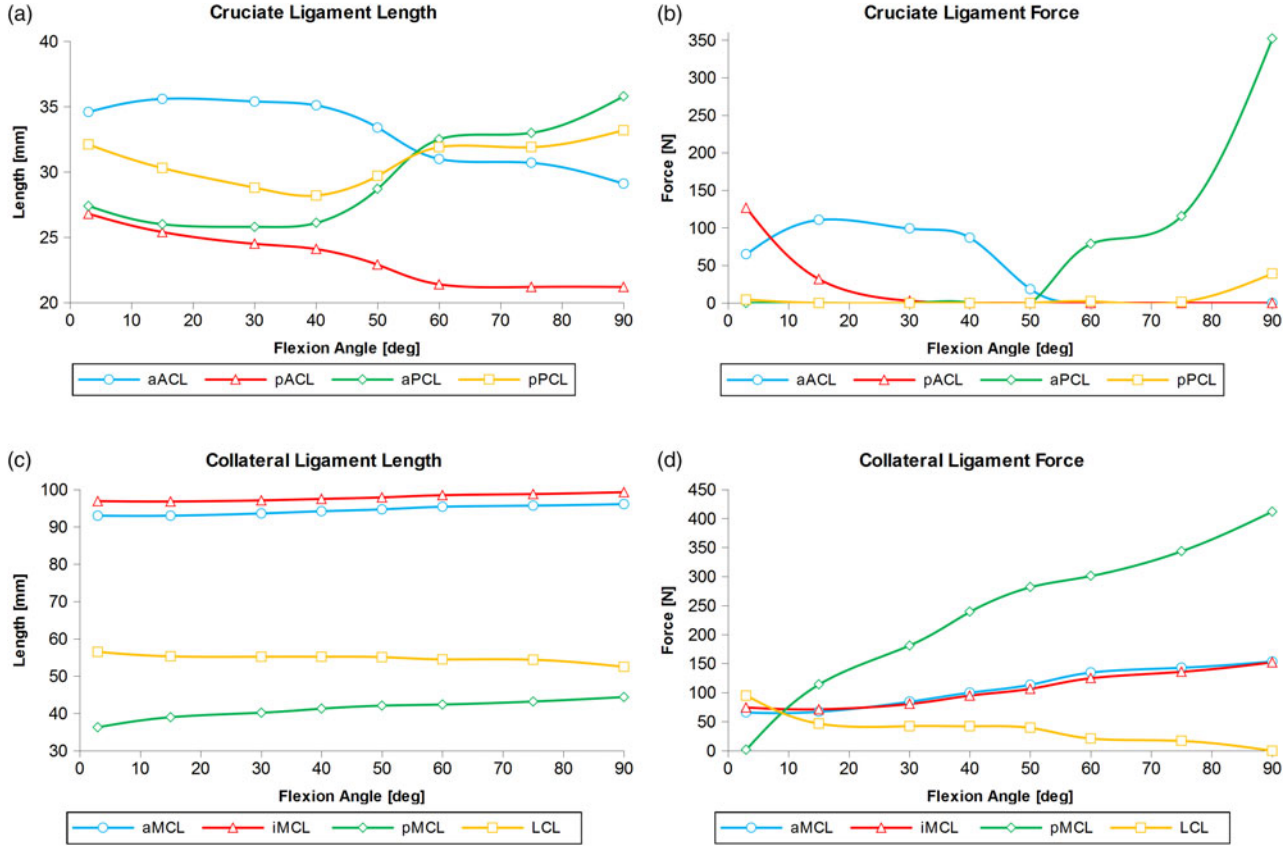

Figure 5. Ligament lengths and forces along the squat movement. (a, b) Four bundles of the cruciate ligaments: aACL and pACL, anterior and posterior portion of the ACL; aPCL and pPCL, anterior and posterior portion of the PCL. (c, d) Collateral ligaments: aMCL and iMCL, anterior and intermediate superficial bundle of MCL; dMCL, deep posterior portion of the MCL; LCL, lateral collateral ligament.

Our results are consistent with data available in literature. Quadriceps force required to keep balance at different squat angles was similar to that obtained *in vivo* by Sharma et al. (2008). Particularly, at 90° of flexion, they report a force of 3 BW while our result was 3.23 BW. Ligament length patterns are comparable to the ones reported by Bergamini et al. (2011). At 90° of flexion the aACL presents a decrease of 15.9% of the reference length. This is in line with measurements obtained *in vivo* (Hosseini et al. 2009; Yoo et al. 2010). Concerning the PCL, our results are in agreement with *in vivo* studies of Li et al. (2004) and DeFrate et al. (2004) that reported an elongation of the PCL bundles. The LCL was found to shorten, consistently with the pattern shown by Bergamini and co-authors and by *ex vivo* studies of Harfe et al. (1998). The aMCL and iMCL in our model showed a gradual elongation, increasing 3.2% and 2.4%, respectively, which favourably compares with the 4% length increase for the MCL reported by Bergamini et al. Finally, the dMCL length increased significantly, particularly in the angle range 0–30°, which concurs with the pattern and values discussed by the above-mentioned authors.

The study of ligament forces is motivated by the high incidence of knee ligament injuries. A more accurate knowledge of the forces experienced by these soft tissues could improve the design and implantation of artificial ligaments and help optimizing ligament reconstruction and ligament balancing during total knee arthroplasty (Fishkin et al. 2002). The ACL and PCL force patterns extracted during the squat motor task well reflect those ones reported by Shelburne and Pandy (1997), although their work considered a planar model. Also consistent with data reported by Shelburne and Pandy (1997) are our data referring to the anterior–posterior drawer. Similarly to these authors, we obtained a resistant force in the order of 200–300 N for a tibia shift of ±5 mm. The anterior and posterior bundles of the PCL exhibited a force trend in agreement with their results. Our peak values of about 300 and 75 N, respectively, are also consistent with experimental data provided by Jurist and Otis (1985) and Hirokawa et al. (1992). An interesting feature is the complementary force pattern of the two main bundles of the cruciate ligaments, with aACL deactivation near 60° of flexion in conjunction with aPCL activation. Reference lengths and elongation patterns of the two superficial bundles of the MCL are in agreement with the previously discussed work of Bergamini and co-authors; combining forces generated by these bundles it is possible to successfully compare our MCL force data with the results obtained by Yang et al. (2010), who found experimental force–stretch curves for the collateral ligaments. Despite the comparable MCL force pattern results, the LCL force trend does not match with the computational data extracted from our model. Indeed, our results are generally higher, probably due to the stiffness and reference strain values set for this ligament.

Previous studies reporting TF force (Nagura et al. 2006; Smith et al. 2008) have obtained a range from 3.73 to 6.2 BW. Bergmann group (Kutzner et al. 2010) has reported *in vivo* measurements in the range 2–3.5 BW, depending on the analysed movement. As reference, Innocenti et al. (2011) reported an average contact force of 3.2–3.7 BW at 90° of flexion. Our result (4.2 BW) is in agreement with these data. Of course, when considering real-world exercises, the activation of other muscles than the knee extensors, had to be considered, that could change the load applied to the internal structures of the knee. The addition of knee flexors but also hip extensors, hip abductors and ankle plantar flexors would help obtaining more realistic results when simulating complex movements, like for example walking or stair climbing. These applications are further objectives of our study.

In conclusion, despite some mismatches with respect to different published data, due to different approximations in the structural components, our numerical values are in agreement with literature. The next stage in our research could be the use of the model to simulate different exercises based on kinematic data obtained from movement analysis. This would enable a detailed analysis of the loads on soft tissues and bones, which would be of great benefit for defining the most suitable parameters for knee prosthesis design and surgery.

Disclosure statement

No potential conflict of interest was reported by the authors.

Notes

1. Email: valerio.sansone@unimi.it
2. Email: carlo.frigo@polimi.it

References

Abdel-Rahman EM, Hefzy MS. 1998. Three-dimensional dynamic behaviour of the human knee joint under impact loading. Med Eng Phys. 20(4):276–290. doi:10.1016/S1350-4533(98)00010-1.

Andriacchi TP, Mikosz RP, Hampton SJ, Galante JO. 1983. Model studies of the stiffness characteristics of the human knee joint. J Biomech. 16(1):23–29. doi:10.1016/0021-9290(83)90043-X.

Bei Y, Fregly BJ. 2004. Multibody dynamic simulation of knee contact mechanics. Med Eng Phys. 26(9):777–789. doi:10.1016/j.medengphy.2004.07.004.

Beillas P, Papaioannou G, Tashman S, Yang KH. 2004. A new method to investigate *in vivo* knee behavior using a finite element model of the lower limb. J Biomech. 37(7):1019–1030. doi:10.1016/j.jbiomech.2003.11.022.

Bendjaballah MZ, Shirazi-Adl A, Zukor DJ. 1995. Biomechanics of the human knee joint in compression: reconstruction, mesh generation and finite element analysis. Knee. 2(2):69–79. doi:10.1016/0968-0160(95)00018-K.

Bergamini E, Pillet H, Hausselle J, Thoreux P, Guerard S, Camomilla V, Cappozzo A, Skalli W. 2011. Tibio-femoral joint constraints for bone pose estimation during movement using multi-body optimization. Gait Posture. 33(4):706–711. doi:10.1016/j.gaitpost.2011.03.006.

Blankevoort L, Huiskes R. 1991. Ligament–bone interaction in a three-dimensional model of the knee. J Biomech Eng. 113(3):263–269. doi:10.1115/1.2894883.

Brunner R, Dreher T, Romkes J, Frigo C. 2008. Effects of plantarflexion on pelvis and lower limb kinematics. Gait Posture. 28(1):150–156. doi:10.1016/j.gaitpost.2007.11.013.

Clauser CE, McConville JT, Young JW. 1969. Weight, volume, and centre of mass of segments of the human body. AMRL technical report (TR-69-70). OH: Wright-Patterson Air Force Base.

DeFrate LE, Gill TJ, Li G. 2004. *In vivo* function of the posterior cruciate ligament during weightbearing knee flexion. Am J Sports Med. 32(8):1923–1928. doi:10.1177/0363546504264896.

Fishkin Z, Miller D, Ritter C, Ziv I. 2002. Changes in human knee ligament stiffness secondary to osteoarthritis. J Orthop Res. 20(2):204–207. doi:10.1016/S0736-0266(01)00087-0.

Frigo C, Pavan EE, Brunner R. 2010. A dynamic model of quadriceps and hamstrings function. Gait Posture. 31(1):100–103. doi:10.1016/j.gaitpost.2009.09.006.

Gill HS, O'Connor JJ. 1996. Biarticulating two-dimensional computer model of the human patellofemoral joint. Clin Biomech (Bristol, Avon). 11(2):81–89. doi:10.1016/0268-0033(95)00021-6.

Harfe DT, Chuinard CR, Espinoza LM, Thomas KA, Solomonow M. 1998. Elongation patterns of the collateral ligaments of the human knee. Clin Biomech. (Bristol, Avon). 13(3):163–175. doi:10.1016/S0268-0033(97)00043-0.

Hirokawa S, Solomonow M, Lu Y, Lou ZP, D'Ambrosia R. 1992. Anterior–posterior and rotational displacement of the tibia elicited by quadriceps contraction. Am J Sports Med. 20(3):299–306. doi:10.1177/036354659202000311.

Hosseini A, Gill TJ, Li G. 2009. *In vivo* anterior cruciate ligament elongation in response to axial tibial loads. J Orthop Sci. 14(3):298–306. doi:10.1007/s00776-009-1325-z. Innocenti B, Pianigiani S, Labey L, Victor J, Bellemans J. 2011. Contact forces in several TKA designs during squatting: a numerical sensitivity analysis. J Biomech. 44(8):1573–1581. doi:10.1016/j.jbiomech.2011.02.081.

Insall JN, Kelly M. 1986. The total condylar prosthesis. Clin Orthop Relat Res. 205:43–48.

Jurist KA, Otis JC. 1985. Anteroposterior tibiofemoral displacements during isometric extension efforts: the roles of external load and knee flexion angle. Am J Sports Med. 13(4):254–258. doi:10.1177/036354658501300407.

Koehle MJ, Hull ML. 2008. A method of calculating physiologically relevant joint reaction forces during forward dynamic simulations of movement from an existing knee model. J Biomech. 41(5):1143–1146. doi:10.1016/j.jbiomech.2007.11.020.

Kutzner I, Heinlein B, Graichen F, Bender A, Rohlmann A, Halder A, Beier A, Bergmann G. 2010. Loading of the knee joint during activities of daily living measured *in vivo* in five subjects. J Biomech. 43(11):2164–2173. doi:10.1016/j.jbiomech.2010.03.046.

Lane NE, Thompson JM. 1997. Management of osteoarthritis in the primary-care setting: an evidence-based approach to treatment. Am J Med. 103(6):S25–S30. doi:10.1016/S0002-9343(97)90005-X.

Li G, DeFrate LE, Sun H, Gill TJ. 2004. *In vivo* elongation of the anterior cruciate ligament and posterior cruciate ligament during knee flexion. Am J Sports Med. 32(6):1415–1420. doi:10.1177/0363546503262175.

Li G, Suggs J, Gill T. 2002. The effect of anterior cruciate ligament injury on knee joint function under a simulated muscle load: a three-dimensional computational simulation. Ann Biomed Eng. 30(5):713–720. doi:10.1114/1.1484219.

Nagura T, Matsumoto H, Kiriyama Y, Chaudhari A, Andriacchi TP. 2006. Tibiofemoral joint contact force in deep knee flexion and its consideration in knee osteoarthritis and joint replacement. J Appl Biomech. 22:305–313.

Papaioannou G, Nianios G, Mitrogiannis C, Fyhrie D, Tashman S, Yang KH. 2008. Patient-specific knee joint finite element model validation with high-accuracy kinematics from biplane dynamic Roentgen stereogrammetric analysis. J Biomech. 41(12):2633–2638. doi:10.1016/j.jbiomech.2008.06.027.

Riener R, Rabuffetti M, Frigo C. 2002. Stair ascent and descent at different inclinations. Gait Posture. 15(1):32–44. doi:10.1016/S0966-6362(01)00162-X.

Sharma A, Leszko F, Komistek RD, Scuderi GR, Cates, Jr, HE, Liu F. 2008. *In vivo* patellofemoral forces in high flexion total knee arthroplasty. J Biomech. 41(3):642–648. doi:10.1016/j.jbiomech.2007.09.027.

Shelburne KB, Pandy MG. 1997. A musculoskeletal model of the knee for evaluating ligament forces during isometric contractions. J Biomech. 30(2):163–176. doi:10.1016/S0021-9290(96)00119-4.

Shrive NG, Frank CB. 2005. Biological materials – articular cartilage. In: Nigg B, Herzog W, editors. Biomechanics of the musculo-skeletal system. 2nd ed.. Chichester: Wiley; p. 92–93.

Smith SM, Cockburn RA, Hemmerich A, Li RM, Wyss UP. 2008. Tibiofemoral joint contact forces and knee kinematics during squatting. Gait Posture. 27(3):376–386. doi:10.1016/j.gaitpost.2007.05.004.

Taylor SJ, Walker PS. 2001. Forces and moments telemetered from two distal femoral replacements during various activities. J Biomech. 34(7):839–848. doi:10.1016/S0021-9290(01)00042-2.

Thompson JA, Hast MW, Granger JF, Piazza SJ, Siston RA. 2011. Biomechanical effects of total knee arthroplasty component malrotation: a computational simulation. J Orthop Res. 29(7):969–975. doi:10.1002/jor.21344.

Yang Z, Wickwire AC, Debski RE. 2010. Development of a subject-specific model to predict the forces in the knee ligaments at high flexion angles. Med Biol Eng Comput. 48(11):1077 – 1085. doi:10.1007/s11517-010-0653-7.

Yoo YS, Jeong WS, Shetty NS, Ingham SJ, Smolinski P, Fu F. 2010. Changes in ACL length at different knee flexion angles: an *in vivo* biomechanical study. Knee Surg Sports Traumatol Arthrosc. 18(3):292–297. doi:10.1007/s00167-009-0932-8.